Proceedings of the 21st ICSMGE, Vienna, Austria, 14 – 19 June 2026. Pistrol, Adam & Schweiger (eds.)
Published by: ÖGG, Austrian Society for Geomechanics, Salzburg, Austria, ISBN 978-3-9503898-4-5
https://doi.org/10.53243/ICSMGE2026-709

Hydromechanical numerical modeling of climate change impacts on earthen dam stability and reservoir dynamics

Amanda Sampaio, Yuderka Trinidad González, Vernon R. Schaefer
Dept. of Civil, Construction, and Environmental Engineering, Iowa State Univ., Ames, IA, ascc@iastate.edu

ABSTRACT: As climate change intensifies precipitation and temperature variability, understanding its effects on reservoir dynamics and dam safety is critical for sustainable water resource management. This study investigates how shifting climate patterns influence the stability of earthen dams, focusing on fluctuations in reservoir levels. For this purpose, hydromechanical numerical modeling is conducted to simulate dam behavior under historical and projected climate scenarios, integrating key variables such as air temperature, precipitation, humidity, and wind speed. In addition, dynamic changes in water flow and saturation levels induced by fluctuating weather patterns are considered by conducting a transient analysis. The study focuses on hydraulic evaluations and stability analysis, particularly considering the evolution of seepage flow and pore-water pressure within the dam structure, and changes in strength reduction factors over time. Results demonstrate that traditional modeling approaches neglecting climate boundary conditions artificially inflate safety factors by 15-25%, providing optimistic predictions. Increased precipitation scenarios produce the most critical conditions, with large climate-induced deformations and lowest strength reduction factors, while decreased precipitation scenarios yield the smallest displacements but remain vulnerable during rapid rewetting transitions. By evaluating how these factors evolve under changing climate conditions, this study provides valuable insights into potential risks to dam integrity, such as internal erosion and excessive pore pressure buildup. This analysis is essential for understanding how earthen dams can withstand the challenges posed by climate change, ensuring their continued effectiveness in flood control and water storage.

KEYWORDS: Earthen Dams, Climate Change, Reservoir Fluctuation, Numerical Modeling.

1 INTRODUCTION

Earthen dams are critical to water resource management providing flood protection, water storage, and hydropower, while accounting for 85% of the number of operational dams in the United States (Billington & Jackson, 2017). However, as climate change increases the frequency and intensity of both floods and droughts, these structures face growing challenges in design, operation, and long-term stability (Sampaio & Trinidad, 2025). In particular, the change in climate patterns promotes rising frequency and intensity of extreme weather events, including prolonged rainfall and seasonal droughts, which are predicted to alter river flows and reservoir level variations (Haider, 2023).

Due to the potential safety risks posed by excessive seepage and elevated pore-water pressures, considerable research has focused on their impact on dam stability. These investigations have sought to quantify pore pressures and seepage rates, as well as to evaluate the effectiveness of different seepage control strategies to enhance the safety of earthen dams (Shuhaib, 2024). Studies also highlight the importance of accounting for climate variability and tidal fluctuations when analyzing earthen structures, as these factors can significantly enhance the accuracy of numerical simulations (Rivera-Hernandez, 2019), and others considered the effects of climate on controlled drawdown scenarios (Sampaio & Trinidad, 2025).

This study uses a numerical modeling approach to evaluate how naturally occurring and projected river and reservoir level fluctuations influence seepage behavior and slope stability in earthen dams. A representative dam geometry and soil profiles were selected to simulate the coupled hydromechanical response under both historical and projected climate conditions. By incorporating land-climate boundary conditions (LCBC), this study captures the interaction between atmospheric variables, temperature, precipitation, solar radiation, and the dam's surface, providing a dynamic representation of seepage and stability over time.

The objective is to assess how natural water level fluctuations, when combined with surface climate interactions, affect the internal pore-water pressure distribution and overall stability of earthen dams under changing climate conditions.

2 MATERIALS AND METHODS

2.1 Study Area and dam description

The Midwest of the United States is characterized by a variable climate, with significant seasonal changes in temperature, frequent and intense precipitation events, and substantial river flow fluctuations (Haider, 2023). As a result, many rivers and reservoirs in this region are subject to rapid hydrologic changes that can cause critical floods and influence the stability of hydraulic structures such as earthen dams (Nilsson, 2020). One such system is the Des Moines River Basin, which exhibits pronounced discharge variability throughout the year. Flows typically peak in late spring due to snowmelt and intensify again during summer storms, while low-flow periods often occur in late summer and early fall (USGS, 2023).

For this study, the Saylorville Dam, located on the Des Moines River near Polk City, Iowa (Figure 1), was used as a reference to define a representative earthen dam cross-section. The model features a 33 m high trapezoidal embankment with a 13 m crest and 340 m base width, these dimensions were simplified from the actual structure while preserving realistic slope geometries (USACE, 2004). This area was also used to model the reservoir level fluctuation based on historical data of gauge reading and water discharge taken from the U.S. Geological Survey (USGS) and the National Oceanic and Atmosphere Administration (NOAA). Figure 1 also shows a sketch of the model used in the simulations.

The soil profile for the embankment was defined based on typical stratigraphy found within the Des Moines Lobe, incorporating representative materials observed across the region. The embankment was modeled as a homogeneous zone composed of compacted silty clay, consistent with local glacial till deposits and selected for its low permeability and cohesive strength (USACE, 2004). The Dam has a granular horizontal and vertical filter, composed of sand, that was previously included in the downstream and center of the embankment to manage seepage and prevent internal erosion. The foundation consists of two stratified layers: an upper silty sand deposit, representing permeable outwash or alluvial material, and a

lower glacial till layer with low permeability and moderate strength (NRCS, 2006; Anderson & Fields, 2009).

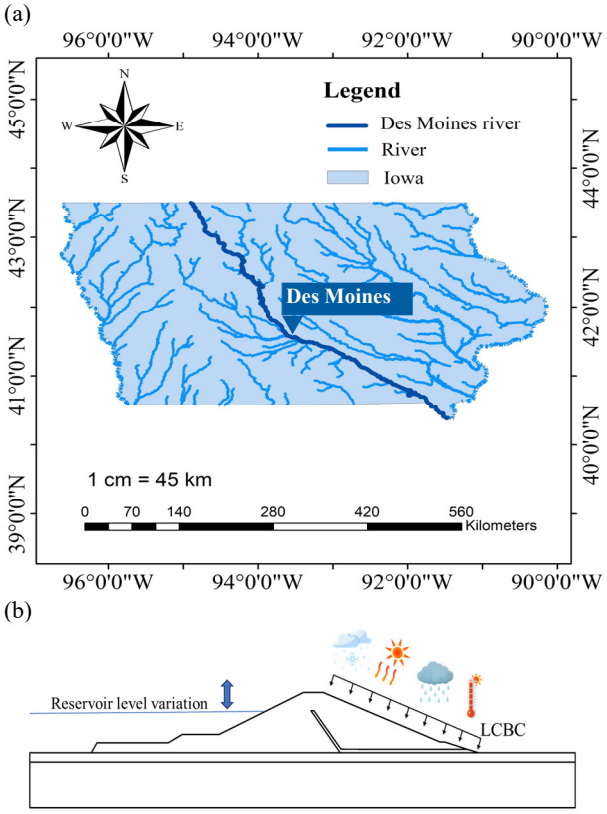

Figure 1. (a) Study Area: Des Moines River (b) Dam Geometry and Land-Climate Boundary Condition.

Key inputs used in the numerical simulations are summarized in Table 1, including material properties for the embankment zones, saturated and residual volumetric water contents, unit weights, shear strength parameters, elastic parameters and hydraulic conductivities.

Table 1. Material properties description

Material Properties	Embankment	Filter	Upper Foundation	Lower Foundation
Saturated ***Kx*** (m/s)	1e-07	1e-02	1e-05	1e-07
Saturated water content	0.35	0.25	0.3	0.35
Residual Vol. water content	0.2	0	0	0.15
Cohesion (kPa)	30	0	5	20
Friction angle	20	38	30	25
Elastic Modulus (MPa)	40	100	50	30
Poisson's ratio	0.35	0.3	0.25	0.45

2.2 Climate variability

An LCBC (Land-Climate Boundary Condition) was defined to capture the influence of climatic variations on the downstream face of the dam. This boundary condition incorporated factors such as air temperature, albedo, solar radiation, snowfall, relative humidity, and precipitation. A continuous three-year record was considered. Seasonal stratification (winter–spring–summer–fall) was applied to compare reservoir levels, seepage response, and stability metrics, noting the heightened summer precipitation variability reported by Robinson (1997). Although multiple climatic variables influence weather behavior, Robinson (1997) emphasizes that temperature and precipitation changes are the most critical when assessing climate impacts. To measure the LCBC effects, a no-boundary scenario [1] was first created, not considering any climate effects on the structure.

The historical climatic and hydrologic variability was simulated based on a 10-year historical dataset of temperature, precipitation, and reservoir levels collected from NOAA and CoCoRaHS weather stations located near the Saylorville Dam. The datasets were processed to simulate a representative three-year period. A Python script generated randomized daily climate sequences while preserving the original mean (within 1%) and standard deviation (within 5%), yielding a statistically consistent baseline dataset for defining the LCBC from historical records [2].

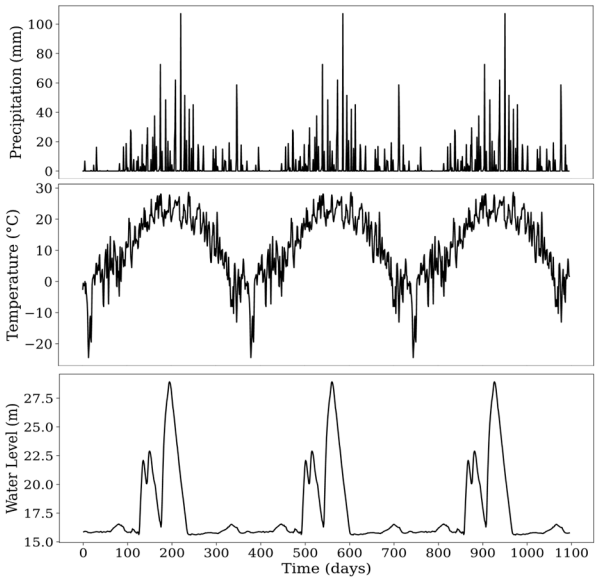

Figure 2. Figure 2. Historical records for the climate variables used to define the LCBC over the analysis period (a) precipitation; (b) temperature; (c) water level.

In addition to atmospheric data, the analysis integrates observed river flow variability as a transient upstream boundary condition. Daily discharge records from USGS and pool depth from NOAA at the Saylorville Reservoir on the Des Moines River were used to simulate the dataset of reservoir levels for the same period. These profiles capture naturally occurring water level changes, including seasonal rise and fall due to snowmelt, storm events, and dry periods.

To assess future climate impacts, two projection scenarios were created based on established regional trends (Easterling, 2017) a drier scenario [3] with a 10% reduction, and a wetter scenario [4], with a 20% increase in precipitation intensity and frequency. An average temperature increase of 4°F was applied to both future datasets according to studies predictions (Kunkel, 2013). These modified datasets represent plausible changes in surface conditions due to climate change and were used to drive simulations of surface-atmosphere interaction and subsurface flow behavior.

For the reservoir levels, the two different scenarios (wetter and drier) were also considered, since reservoir fluctuations are directly associated with rainfall. In the wetter scenario, levels were increased to reflect the projected 20-30% rise in heavy precipitation events and higher spring runoff across the Midwest (Schilling & Wolter, 2016), including short-term peaks to simulate possible flooding. The drier scenario lowered levels to represent reduced summer inflows and higher

evapotranspiration, as projected by the USGCRP (2018). Figure 2. Shows the historical records for the climate variables used to define the LCBC over the analysis period.

2.3 Numerical modeling framework

Seepage and stability issues can be addressed by many methods, which can be classified as analytical, experimental, or numerical. This study conducted numerical modeling based on finite elements. Specifically, SEEP/W and SIGMA/W, GeoStudio, were used for the analyses.

SEEP/W was used to model transient seepage under unsaturated-saturated conditions parameterized by the measured soil-water retention curve, solving the governing flow equations via the finite element method through the Galerkin-weighed residual formulation (Zienkiewicz, 1967). The total water flux through the dam body was modeled using Darcy's Law, incorporating both vertical and horizontal flow components, with time-dependent reservoir boundary conditions. A more detailed discussion of this method was described by Sampaio & Trinidad (2025).

Deformation analyses were performed in SIGMA/W, the finite-element module of GeoStudio for modeling stress–strain behavior in soil structures under mechanical and hydraulic loading. Coupled hydromechanical effects were represented by importing time-varying pore-water pressure fields from SEEP/W simulations for each climate scenario. This setup enabled simulation of how changes in seepage patterns drive deformation within the embankment and foundation. Soil behavior was represented with a Mohr–Coulomb constitutive model using zone-specific strength parameters.

In addition to the deformation assessment, a strength-reduction factor (SRF) analysis, i.e., the shear strength reduction (SSR) method, was conducted in SIGMA/W to estimate the factor of safety for each scenario at given times. In this procedure, the Mohr–Coulomb strength parameters are uniformly scaled by a factor F ($c' \rightarrow c'/F$, $\tan\varphi' \rightarrow \tan\varphi'/F$) and progressively reduced until numerical non-convergence and/or runaway deformations indicate incipient failure; the reduction factor at this limit state is taken as the factor of safety (Zienkiewicz et al., 1975; Griffiths & Lane, 1999; Dawson et al., 1999). Following the simulations, contours were examined to characterize spatial variations in pore-pressure fields, seepage patterns through the dam body, and deformation of the embankment and foundation.

To track how stability evolves through time, the SRF was evaluated at multiple time slices bracketing major flooding events across the three-year period for each climate scenario. Time instants were selected immediately before the hydrograph rise (pre-event), at or near peak pore-water pressure (peak), and during the recession limb (post-event). For each slice, the imported pore-pressure field was fixed while the Mohr–Coulomb strength parameters were uniformly reduced until non-convergence; the corresponding reduction factor was recorded as the factor of safety.

3 RESULTS

3.1. Pore-water pressure

Figure 3 shows the PWP analysis results through a temporal evolution and a set of contour visualizations for the dam under different boundary conditions. Figure 3(a) shows the development of the cumulative PWP over a 3-year simulation period under the four different boundary condition scenarios: [1] no boundary conditions, [2] historical climate conditions, [3] decreased precipitation, and [4] increased precipitation. Figure 3(b) presents PWP contours for the same four scenarios at the end of the simulation. Results from Figure 3 (a) show that as expected, scenario [4] (increased precipitation), produces the largest positive PWP peaks during flood stages and the highest wet antecedent baseline between events, indicating sustained elevation of the phreatic surface and slower dissipation. Scenario [2] (historical) tracks lower than [4] with moderate peaks and steadier inter-event recovery. Scenario [3] (decreased precipitation) shows the smallest amplitudes and the flattest baseline; prolonged drying raises matric suction, so effective stress remains higher and post-event PWP decays quickly.

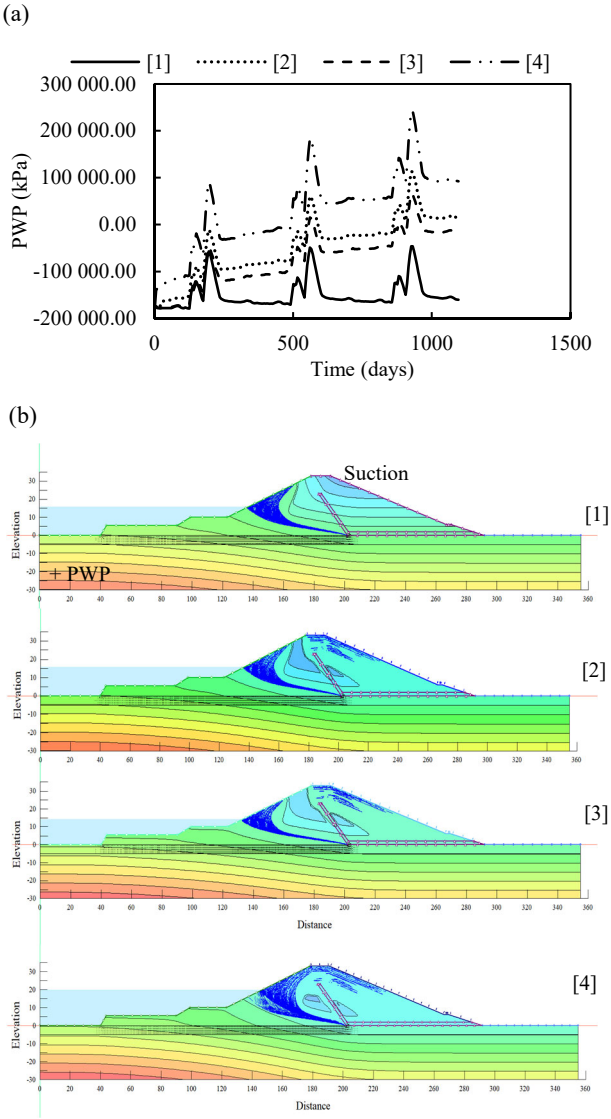

Figure 3. (a) comparison of PWP variation through time for different climate conditions near the entrance of the filter (b) Pore water pressure contours observed in the dam at the end of the simulation under different climate conditions [1], [2], [3] and [4].

Scenario [1] (no climate boundary) exhibits a persistently negative PWP (suction) with brief upward excursions, reflecting the absence of realistic hydroclimatic loading; it is a best-case, nonphysical baseline that suppresses transients. Overall, [4] yields the most critical short-term conditions immediately during and after floods (largest positive PWP spikes and delayed recovery), whereas [3] is comparatively stable with limited fluctuation. For risk considerations, case [4] governs flood-driven PWP spikes, and a higher wet baseline depress effective stress, elevate the phreatic surface, and prolong recovery, conditions that heighten likelihood of downstream-slope instability, toe uplift, and internal erosion along the core–filter contact. The contours in Figure 3(b) show

that the most notable differences among scenarios occur in the distribution and extent of suction zones near the filter and core–filter interface, rather than large-scale changes in deep positive PWP fields. In scenario [4], suction around the filter is reduced, indicating wetter conditions that lower effective stress locally and can make the filter zone more susceptible to internal erosion or backward erosion piping if gradients rise during flood events. The historical scenario [2] shows slightly greater suction retention than [4], suggesting a modestly drier and more stable interface. In the decreased-precipitation [3], suction zones around the filter are more extensive and persistent, reflecting a drier state that increases effective stress and reduces the likelihood of hydraulic connectivity through the core–filter contact. The no-climate-boundary case [1] displays the largest and most uniform suction region, an idealized condition unlikely to occur in practice. These contour patterns imply that stability risk is controlled more by loss of suction near critical interfaces, with [4] representing the highest susceptibility during and after flood events.

3.2. Seepage

Figure 4 shows seepage contours at (a) end of year 1 and (b) end of the final year, for scenarios [1] – [4].

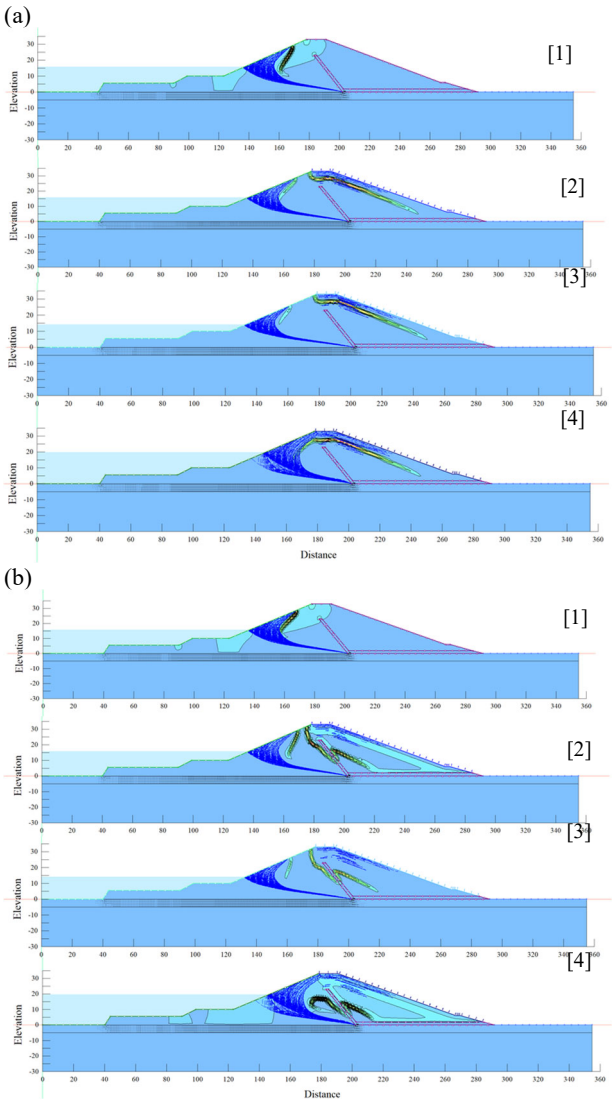

Figure 4. Seepage behavior under different climate scenarios. (a) Seepage contours at the end of the first year under different climate conditions [1], [2], [3] and [4]. (b) Seepage contours at the end of last year under different climate conditions [1], [2], [3] and [4].

The no-boundary case [1] displays a comparatively low phreatic surface and short flow paths with gentle gradients, an optimistic baseline that suppresses climate–driven transients. Relative to [1], both [2] and [4] show a higher phreatic surface and a thicker saturated wedge within the core and downstream shell; this effect is most pronounced in [4], where denser, tightly spaced contours extend toward the downstream toe and along the core–filter contact, indicating larger seepage flux and steeper exit gradients. [3] presents the opposite tendency: a depressed phreatic line and smaller positive-pressure bulbs, yielding gentler gradients and shorter flow paths through the core/foundation interface.

Comparing year 1 (a) to the last year (b), cumulative wetting in [4] sustains or expands the saturated zone and keeps gradients elevated, whereas [3] maintains a contracted seepage envelope with limited growth over time; [2] remains intermediate. Taken together, the contour patterns identify [4] (increased precipitation) as the critical condition for seepage-driven hazards, internal erosion/piping at the core–filter contact and high exit gradients at the downstream toe, while [3] (decreased precipitation) is the least demanding steady condition, noting that drawdown/rewet transients (not captured in these end-of-year snapshots) still warrant operational caution.

3.3. Displacement

Figure 5 displays XY-displacement contours at the end of the 3-year simulation for scenarios [1] – [4]. Deformation localizes at the crest (settlement) and along the downstream shell and toe (outward translation), with secondary bands near the core–filter contact. Each panel displays the spatial distribution of total displacement magnitudes within the earthen structure cross-section, with contour lines representing zones of equal displacement. The color gradient progresses from blue/light (minimal displacement) through green and yellow to red (maximum displacement), providing a visual representation of deformation patterns.

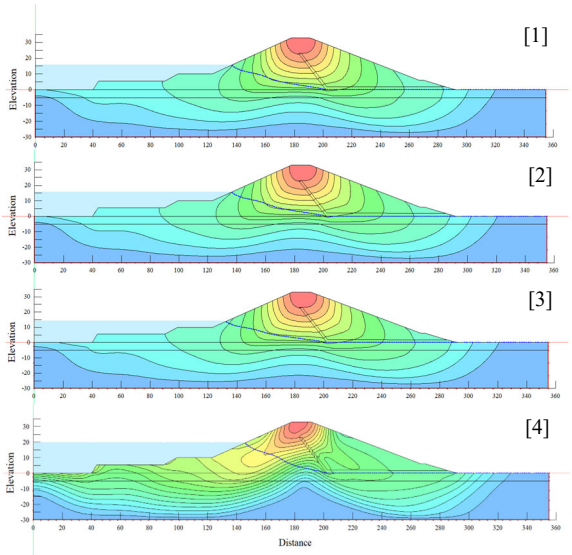

Figure 5. XY-displacement contours for all four scenarios at the at the end of last year under different climate conditions [1], [2], [3] and [4].

The no-boundary case [1] shows a largest peak at the top of the embankment, on the other hand, increased precipitation [4] shows the greatest climate-induced deformations, with a broad up and downstream zones and crest settlement approaching [1], consistent with elevated phreatic levels and reduced stiffness. Historical conditions [2] are intermediate, while decreased precipitation/drawdown [3] yields the smallest and most

confined displacements, reflecting suction-induced stiffening under drier states.

Figure 6 shows the variation of the SRF over time for the three-year period, sampled at specific intervals before and after major flooding and drought events. Results are shown for the four climate scenarios: [1] no climate boundary, [2] historical climate, [3] decreased precipitation, and [4] increased precipitation. Scenario [1] consistently yields the highest SRF values; however, this represents an idealized, best-case baseline in which climate boundaries are excluded. By neglecting pore-water-pressure transients and other hydro-climatic interactions, this configuration produces an artificially elevated stability response that does not reflect real-world performance. Once climate forcing is included, SRF decreases relative to [1].

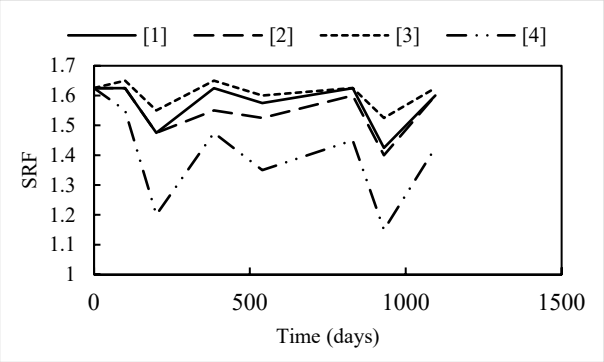

Figure 6. SRF vs. time over a 3-year simulation, sampled before/after major flooding and drought events, for four climate scenarios: [1] no climate boundary, [2] historical, [3] decreased precipitation, and [4] increased precipitation.

Scenario [3] maintains the highest SRF with the smallest fluctuations, indicating a more stable condition: sustained small drying events elevates matric suction, increase effective stress, and dampens pore-pressure transients, so SRF remains comparatively high through events. For scenario [4] (increased precipitation), SRF is the lowest overall. Before flooding, antecedent wetness keeps the baseline SRF depressed relative to the other scenarios. During and immediately after flood peaks, infiltration and elevated reservoir stages drive sharp pore-water-pressure rises, reducing effective stress and producing the largest SRF drops; recovery is delayed until dissipation restores gradients. These responses identify post-flood periods in [4] as the most critical windows for stability.

Event-scale SRF changes in Figure 6 quantify the sensitivity to floods: the idealized no-boundary case [1] drops only ~5–8% and rebounds within ~0–2%, the historical case [2] declines ~7–10% with a near-full recovery (~1–3%), and the decreased-precipitation scenario [3] shows the smallest dips (~3–6%) with rapid rebound (±1–2%). In contrast, increased precipitation [4] exhibits the deepest reductions (~15–25%) and the slowest recovery, often remaining ~5–10% below pre-event levels for a period. These percentages indicate the need for robust, event-aware prediction models that explicitly account for extreme precipitation and delayed dissipation, quantifying residual SRF deficits and recovery times, especially for embankments near the stability–failure boundary, where [4]-type events can tip the system into instability.

3.1 Risk considerations

The findings from this comprehensive hydromechanical analysis reveal critical risk considerations that should inform best practices for numerical modeling of climate-sensitive earthen structures. The underestimation of deformation and stability risks in the no-boundary scenario (Scenario 1) demonstrates that traditional geotechnical modeling approaches that neglect climate variables can lead to unsafe designs, with strength reduction factors artificially inflated by 15-25% compared to realistic climate-aware scenarios. This bias toward optimistic predictions highlights a flaw in conventional practice where climate forcing is treated as negligible rather than as a primary design driver. For robust numerical modeling practice, engineers must incorporate transient land-climate boundary conditions (LCBC) that capture the full spectrum of atmospheric interactions, including temperature fluctuations, precipitation variability, and seasonal cycles, as these directly influence pore-water pressure evolution and material behavior over time. The identification of Scenario 4 (increased precipitation) as governing serviceability and stability risks highlights the necessity of conducting probabilistic analyses using projected extreme climate scenarios rather than relying solely on historical records, particularly given that post-flood recovery periods exhibit prolonged strength deficits that may not fully restore pre-event safety margins.

The temporal sensitivity revealed through SRF monitoring emphasizes that static end-of-construction or steady-state analyses are insufficient for climate-exposed infrastructure, requiring instead continuous transient modeling with event-scale resolution to capture critical vulnerability windows during and immediately following extreme weather events. Actionable best practices should therefore mandate: (i) implementation of transient land-climate boundary conditions that capture temperature, precipitation, and seasonal cycles together with realistic reservoir hydrographs; (ii) resolution of unsaturated-saturated seepage with measured soil-water retention curves and calibrated conductivities, ensuring mesh and time-step convergence while validating dissipation rates; (iii) evaluation of stability through event-aware SRF analysis at pre-peak, peak, and post-event intervals, reporting both ΔSRF magnitude and recovery time as actionable design metrics; (iv) explicit modeling of critical interfaces such as core-filter contacts and downstream toes where suction loss governs failure mechanisms; (v) probabilistic uncertainty bracketing through ensemble modeling of wetter/drier climate futures and rapid drawdown/rewetting scenarios; and (vi) assessment of cumulative damage effects from repeated climate loading cycles over multi-year operational sequences. These practices could ensure that numerical predictions adequately reflect field performance under changing environmental conditions and support climate-resilient infrastructure design decisions, particularly for embankments operating near the stability-failure boundary where climate-induced perturbations can trigger cascading failure modes.

4. CONCLUSION

This study demonstrates that climate boundary conditions fundamentally alter earthen dam behavior, with traditional no-climate modeling providing optimistic stability predictions that underestimate real-world performance by up to 25%. The hydromechanical analysis reveals that increased precipitation scenarios govern critical design conditions through elevated pore-water pressures, enhanced seepage gradients, and prolonged post-event recovery periods that sustain vulnerability windows. While decreased precipitation conditions appear favorable under steady-state analysis, the potential for rapid strength loss during rewetting transitions highlights the importance of transient modeling approaches. These findings underline the need for climate-informed numerical modeling practices that incorporate realistic atmospheric boundary conditions and time-dependent stability assessments to ensure the continued safety and serviceability of earthen infrastructure under changing environmental conditions.

5. ACKNOWLEDGEMENTS

This work was supported by the Department of Civil, Construction, and Environmental Engineering at Iowa State University.

REFERENCES

Anderson, R.R. and Fields, C., eds., 2009. Geology of the Saylorville Spillway: After the Flood of 2008. Geological Society of Iowa Guidebook 84. Iowa City, IA.

Billington, D.P. and Jackson, D.C. (2017) Big Dams of the New Deal Era: A Confluence of Engineering and Politics. Norman, OK: University of Oklahoma Press.

CoCoRaHS - community collaborative rain, hail & snow network (no date) Cocorahs.org. at: https://www.cocorahs.org/ (Accessed: December 12, 2024).

Easterling, D.R. et al. (2017) Ch. 7: Precipitation change in the United States. Climate science special report: Fourth national climate assessment, volume I. U.S. Global Change Research Program.

Dawson, E. M., Roth, W. H., and Drescher, A. (2015). "Slope stability analysis by strength reduction." (January 1999).

Griffins, D. V., and Lane, P. A. (1999). "Slope stability analysis by finite elements." *Geotechnique*, 49(3), 387–403.

Haider, S., Masood, M.U., Rashid, M., Alshehri, F., Pande, C.B., Katipoğlu, O.M. and Costache, R., 2023. Simulation of the potential impacts of projected climate and land use change on runoff under CMIP6 scenarios. *Water*, *15*(19), p.3421.

Kunkel, K.E., Stevens, L.E., Stevens, S.E., Sun, L., Janssen, E., Wuebbles, D., Konrad, C.E., Fuhrman, C.M., Keim, B.D., Kruk, M.C. and Billot, A., 2013. Regional climate trends and scenarios for the US National Climate Assessment: Part 2. Climate of the Southeast US.

National Centers for Environmental Information (NCEI) (no date) Climate Data Online,Noaa.gov. Available at: https://www.ncei.noaa.gov/cdo-web/ (Accessed: December 12,2024).

Nilsson, C. and Berggren, K., 2000. Alterations of riparian ecosystems caused by river regulation: Dam operations have caused global-scale ecological changes in riparian ecosystems. How to protect river environments and human needs of rivers remains one of the most important questions of our time. *BioScience*, *50*(9), pp.783-792.

NRCS (2006) Soil Survey of Polk County, Iowa. United States Department of Agriculture, Natural Resources Conservation Service.

Pryor, S.C. et al. (2014) "Ch. 18: Midwest. Climate Change Impacts in the United States:The Third National Climate Assessment." Edited by J.M. Melillo, G.W. Yohe, and U.S.Global Change Research Program, pp. 418–440.

Pryor, S.C., Barthelmie, R.J. and Schoof, J.T. (2013) "High-resolution projections ofclimate-related risks for the Midwestern USA," Climate research, 56(1), pp. 61–79.Available at: https://doi.org/10.3354/cr01143.

Rivera-Hernandez, X.A., Ellithy, G.S. and Vahedifard, F. (2019) "Integrating fieldmonitoring and numerical modeling to evaluate performance of a levee under climaticand tidal variations," Journal of geotechnical and geoenvironmental engineering,145(10), p. 05019009. Available at: https://doi.org/10.1061/(asce)gt.1943-5606.0002134.

Robinson, P.J., 1997. Modeling utility load and temperature relationships for use with long-lead forecasts. *Journal of Applied Meteorology*, *36*(5), pp.591-598.

Robinson, P.J., 1997. Climate change and hydropower generation. *International journal of climatology: a journal of the Royal Meteorological Society*, *17*(9), pp.983-996.

Sampaio, A. and González, Y.T., Hydromechanical Numerical Modeling Approach for Assessing Climate-Induced Risks on the Stability of Earthen Dams. In *World Environmental and Water Resources Congress 2025* (pp. 48-61).

Schilling, K.E. and Wolter, C.F., 2016. Modeling climate change impacts on streamflow in Iowa watersheds. Journal of Hydrology: Regional Studies, 5, pp.1–14. Available at: https://doi.org/10.1016/j.ejrh.2015.11.002.

U.S. Army Corps of Engineers (USACE), 2004. Engineering and Design – Slope Stability. EM 1110-2-1902. Washington, DC: Department of the Army.

U.S. Geological Survey (USGS) (2023) Peak streamflow trends in Iowa and their relation to changes in precipitation and snowmelt, Scientific Investigations Report 2023–5064 C.

USGCRP, 2018. Impacts, Risks, and Adaptation in the United States: Fourth National Climate Assessment, *Chapter 21: Midwest.* [online] U.S. Global Change Research Program. Available at: https://nca2018.globalchange.gov/chapter/21/ [Accessed 23 May. 2025].

Zienkiewicz, O.C. and Taylor, R.L. (1967) The Finite Element Method; Volumes I. NewYork: McGraw Hill.